Acta Cryst. (1978). B**34**, 3027–3036

X-ray Study of Budesonide: Molecular Structures and Solid Solutions of the (22*S*) and (22*R*) Epimers of 11β,21-Dihydroxy-16α,17α-propylmethylenedioxy-1,4-pregnadiene-3,20-dione

BY JÖRGEN ALBERTSSON, ÅKE OSKARSSON AND CHRISTER SVENSSON

Inorganic Chemistry, Chemical Center, University of Lund, POB 740, *S*-220 07 *Lund* 7, *Sweden*

(*Received* 17 *March* 1978; *accepted* 15 *May* 1978)

The molecular structures of the (22*S*) and (22*R*) epimers of the corticosteroid budesonide, 11β,21-dihydroxy-16α,17α-propylmethylenedioxy-1,4-pregnadiene-3,20-dione, $C_{25}H_{34}O_6$, have been determined by investigating the crystal structures of two compounds containing 92% of the (22*S*) and 8% of the (22*R*) epimer (*A*) and 95% of the (22*R*) and 5% of the (22*S*) epimer (*B*). The X-ray intensities were collected with a four-circle single-crystal diffractometer. *A* and *B* crystallize in space group $P2_12_12_1$ with $Z = 4$: $a = 8{\cdot}550$ (1), $b = 9{\cdot}406$ (1), $c = 28{\cdot}401$ (3) Å for *A*; $a = 8{\cdot}419$ (1), $b = 9{\cdot}087$ (1), $c = 29{\cdot}523$ (4) Å for *B*. The refinements converged to $R = 0{\cdot}067$ (*A*) and 0·059 (*B*). In both epimers rings *B* and *C* have the chair conformation. Ring *D* is a distorted 13β,14α-envelope. The planar ring *A* is bent 40·7° from the bulk of the steroid in the (22*S*) epimer and 43·1° in the (22*R*) epimer. The propyl chain is equatorially oriented to the dioxolane ring in both molecules and it is thus α-axial to the steroid. As a result the two molecules are very similar and can pack together in a crystal. An investigation of single crystals with epimeric composition ranging from 0 to 95% of the (22*R*) epimer shows that the two compounds form a continuous range of solid solutions.

Introduction

The anti-inflammatory corticosteroid budesonide has been prepared and chemically investigated at AB Draco,* Lund, Sweden, by Thalén and co-workers and tested for biological activity by Brattsand and co-workers (Brattsand, Thuresson af Ekenstam, Claeson & Thalén, 1975*a*,*b*; Thalén & Brattsand, 1978). Budesonide is the 16α,17α-acetal of 16α-hydroxyprednisolone with *n*-butyraldehyde. As a new centre of chirality is introduced into the molecule at the C(22) atom, two epimers are possible, (I): (22*S*) and (II): (22*R*) (Fig. 1). Preparative and analytical methods of chromatographic separation of the two epimers have been developed by Thalén, Wikby and co-workers (Thalén & Brattsand, 1978; Brattsand, Thuresson af Ekenstam, Claeson & Thalén, 1975*b*; Wikby, Thalén & Oresten, 1978; Wikby, Nilsson & Hällsås, 1978). Both epimers were found to have unexpectedly high anti-inflammatory activity for non-halogenated corticosteroids.

* Subsidiary to AB Astra, Sweden.

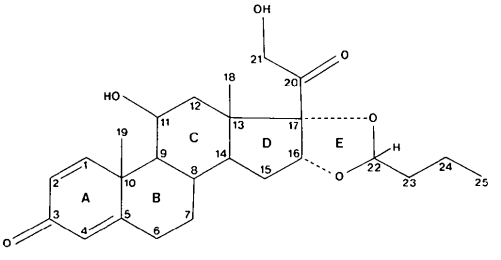

Fig. 1. Budesonide: molecular skeleton of the (22*S*) and (22*R*) epimers and the labelling of the atoms and rings.

As can be inferred from van der Waals models based on Fig. 1, the shapes of the two epimers of budesonide can be very similar if the propyl substituent is equatorial to ring *E*, *i.e.* α-axial to the steroid nucleus (rings *A*–*D*). The other conformations differ more but in (II) the position of the propyl chain axial to ring *E* is hindered by steric interaction with the α H atoms of the nucleus. The conformational freedom of ring *E* and the propyl chain should be important for the chromatographic separation of the two epimers (Wikby, Nilsson & Hällsås, 1978).

In order to establish the correct configurations and the conformations of the two steroid nuclei and their substituents, we have investigated the crystal structures of two preparations (*A* and *B*) of budesonide with single-crystal methods. Preparation *A* contained 92% of epimer (I) and 8% of epimer (II). The corresponding values for *B* were 5 and 95% respectively. It was found that the overall molecular shape as well as the molecular packing were very similar in *A* and *B*. To investigate whether different phases are formed in the binary system of (I) and (II), we also determined the unit-cell dimensions for various preparations ranging from 100% (I), 0% (II) to 5% (I), 95% (II) using single-crystal methods.

Experimental

Six batches of single crystals, differing in their relative amounts of epimers (I) and (II), were grown from various solvents by Thalén & Wickström (1977) as shown in Table 1. All the preparations gave short prismatic crystals which were colourless or very faintly yellow. Preliminary Weissenberg and oscillation photographs showed that both *A* and *B* crystallize in the Laue class *mmm* with the reflexions $h00$: $h \neq 2n$, $0k0$: $k \neq 2n$ and $00l$: $l \neq 2n$ absent. The unit-cell dimensions were determined for two single crystals from each of the six batches. For each crystal 67–69 θ values were measured with a CAD-4 single-crystal diffractometer using Ni-filtered Cu $K\alpha$ radiation ($\lambda = 1{\cdot}540562$ Å) at a take-off angle of 5° and a temperature of 22°C. The method is described by Danielsson, Grenthe & Oskarsson (1976). The relative amounts of (I) and (II) were determined by high-performance liquid chromatography at AB Draco for each of the twelve single crystals. The results are given in Table 1.

The crystal structures were determined for compounds *A* and *B*. Table 2 gives information concerning the crystal data, the collection and reduction of the intensity data sets, and the refinements based on them. During the data collection three standard reflexions were checked after every 100 measurements. No systematic variation in their intensities were detected. The values of I and $\sigma_c(I)$ were corrected for Lorentz, polarization and absorption effects [$\sigma_c(I)$ is based on counting statistics]. The expression used in the polarization correction was $p = (\cos^2 2\theta_M + \cos^2 2\theta)/(1 + \cos^2 2\theta_M)$ with $\theta_M = 13{\cdot}28°$.

The intensities of the reflexions used in the determinations of the unit-cell dimensions were also measured. Ni-filtered instead of graphite-monochromated Cu $K\alpha$ radiation was used since some crystals were rather large. The ω interval in the ω–2θ scan varied from $\Delta\omega = 0{\cdot}8° + 0{\cdot}5° \tan\theta$ to $\Delta\omega = 1{\cdot}2° + 0{\cdot}3° \tan\theta$. The largest interval was used for preparation No. 4 ($x_{II} = 0{\cdot}60$). The minimum number of counts was 2500 and the maximum recording time 5 min. For each batch one small (about 0·2 × 0·2 × 0·2 mm) and one large (about 0·5 × 0·5 × 0·5 mm) crystal were used.

Table 2. *Budesonide A and B: crystal data, collection and reduction of intensities, and the least-squares refinement*

Unit-cell dimensions are given in Table 1.

	A	*B*
Formula	$C_{25}H_{34}O_6$	
FW	430·5	
Crystal system	Orthorhombic	
Space group	$P2_12_12_1$	
Z	4	
D_x (g cm^{-3})	1·25	1·27
Crystal size (mm)	0·30 × 0·10 × 0·20	0·25 × 0·25 × 0·25
Radiation	Graphite-monochromated Cu $K\alpha$	
ω interval (°) (ω–2θ scan)	0·70 + 0·50 tan θ	0·50 + 0·50 tan θ
θ interval (°)	5–70	
Minimum number of counts in a scan	3000	
Maximum recording time (s)	180	
μ (cm^{-1})	6·35	6·45
Range of the transmission factor	0·88–0·94	0·86–0·89
Number of measured reflexions	2490	2456
Number of reflexions given zero weight [$I < 3\sigma(I)$]	820	391
Number of independent reflexions used in the final refinement	1670	2065
$R = \Sigma\|\|F_o\| - \|F_c\|\|/\Sigma\|F_o\|$	0·067	0·059
$R_w = [\Sigma w(\|F_o\| - \|F_c\|)^2/\Sigma w\|F_o\|^2]^{1/2}$	0·095	0·083
$S = [\Sigma w(\|F_o\| - \|F_c\|)^2/(m-n)]^{1/2}$	1·07	0·93
C_1 (weighting function)	0·060	0·055
C_2 (weighting function)	0·4	0·4
g ($\times 10^{-4}$)	0·7 (3)	0·5 (1)
Range of extinction correction on $\|F_o\|$	1·00–1·16	1·00–1·20

Table 1. *The unit-cell dimensions at 22°C and the epimeric compositions of six different batches of budesonide*

The solvent from which each batch of single crystals was grown is given. The mole fraction x_{II} is defined by $x_{II} = n_{II}/(n_I + n_{II})$ where n_I and n_{II} are the amounts of substance of (I) and (II) respectively. The amount of impurities varied between 0 and 3 wt%.

Batch number	Solvent	x_{II}	a (Å)	b (Å)	c (Å)	V (Å^3)
1	Ethyl acetate	0·000	8·538 (1)	9·460 (1)	28·293 (2)	2285·2
		0·000	8·534 (1)	9·454 (2)	28·273 (7)	2281·3
2 (*A*)	Toluene	0·076	8·550 (1)	9·406 (1)	28·401 (3)	2284·0
		0·086	8·553 (1)	9·415 (1)	28·396 (2)	2286·4
3	50% Methanol–50% water	0·294	8·553 (1)	9·278 (1)	28·702 (3)	2277·6
		0·298	8·554 (1)	9·288 (1)	28·695 (3)	2280·1
4	Toluene	0·604	8·513 (1)	9·171 (4)	29·032 (14)	2266·7
		0·606	8·516 (1)	9·194 (2)	29·071 (7)	2276·1
5	Ethanol	0·857	8·442 (1)	9·100 (1)	29·423 (4)	2260·4
		0·862	8·441 (1)	9·121 (1)	29·434 (5)	2266·2
6 (*B*)	Toluene and petroleum ether	0·953	8·419 (1)	9·087 (1)	29·523 (4)	2258·5
		0·952	8·421 (1)	9·094 (2)	29·525 (6)	2261·0

Solution and refinement of the structures

Most non-H atoms in *A* and *B* were located using the program *MULTAN* (Germain, Main & Woolfson, 1971). Difference maps showed that the propyl chain was disordered in both structures with C(23) – C(25) statistically distributed over two positions (denoted *a* and *b* below). When the molecular skeleton had been located, the approximate positions of the H atoms in the CH and the CH_2 groups were calculated from geometrical considerations and included in the two models. Towards the end of each refinement, a difference map revealed the positions of the remaining H atoms except those connected to C(25*a* and *b*) in both *A* and *B* and to O(11) in *B*, which were never located.

The parameters were improved by full-matrix least-squares refinements minimizing $\sum w(|F_o| - |F_c|)^2$ with weights calculated from $w = [\sigma_c^2(|F_o|^2)/4|F_o|^2 + (C_1|F_o|)^2 + C_2]^{-1}$. C_1 and C_2 were adjusted so that constant values of $\langle w(|F_o| - |F_c|)^2 \rangle$ were obtained in different $|F_o|$ and $\sin\theta$ intervals. Anisotropic thermal parameters were assigned to atoms C(1) – C(22) and to the O atoms. Isotropic thermal parameters were used for the disordered atoms C(23) – C(25) and the H atoms. The H atoms connected to C(23) and C(24) were not refined and were given temperature factors = 5·0 Å^2 in *A* and 7·0 Å^2 in *B*. An isotropic extinction parameter (Zachariasen, 1967) was included in both refinements. In both cases only 4% of the reflexions had corrections differing from 1·00.

The final models of *A* and *B* contained 68 atoms and a total of 383 parameters. Therefore, only a part of each model was refined at a time. In the final cycle the parameters of all the non-H atoms were varied. The shifts were less than 50% of the estimated standard deviations. For both *A* and *B* the highest residuals in the final difference map (about 0·3 e Å^{-3}) showed up in the regions of the disordered propyl chains. This disorder may also be the reason why a few of the H atoms have been refined to positions that are obviously unreasonable. The scattering factors used in the calculations were taken from Doyle & Turner (1968) (O and C) and from Stewart, Davidson & Simpson (1965) (H). Table 3 gives the final positional parameters.*

* Lists of structure factors and thermal parameters for both epimers have been deposited with the British Library Lending Division as Supplementary Publication No. SUP 33676 (18 pp.). Copies may be obtained through The Executive Secretary, International Union of Crystallography, 5 Abbey Square, Chester CH1 2HU, England.

Table 3. *Atomic coordinates* ($\times 10^4$, $\times 10^3$ *for* H) *of epimer* (I) *in preparation A of budesonide and of* (II) *in B with estimated standard deviations*

The H atoms connected to C(25) in *A* and *B* and to O(11) in *B* were not located. The occupancy of the propyl-chain atoms is *A*: 0·25(2) (*a*) and 0·75 (2) (*b*); *B*: 0·45 (1) (*a*) and 0·55 (1) (*b*).

	(I) in *A*			(II) in *B*		
	x	*y*	*z*	*x*	*y*	*z*
C(1)	10200 (9)	568 (7)	5781 (2)	10301 (6)	694 (5)	5783 (1)
C(2)	10448 (9)	151 (8)	5336 (2)	10565 (6)	322 (5)	5349 (1)
C(3)	11545 (9)	859 (9)	5039 (2)	11671 (6)	1145 (7)	5065 (2)
C(4)	12331 (8)	2092 (9)	5237 (2)	12511 (6)	2346 (6)	5288 (2)
C(5)	12090 (7)	2565 (8)	5678 (2)	12268 (5)	2739 (6)	5717 (1)
C(6)	12867 (8)	3887 (9)	5870 (3)	13077 (6)	4044 (7)	5913 (2)
C(7)	11701 (8)	4920 (8)	6047 (2)	11847 (5)	5175 (6)	6089 (2)
C(8)	10495 (6)	4287 (7)	6392 (2)	10611 (5)	4491 (5)	6406 (1)
C(9)	9736 (6)	2950 (6)	6165 (2)	9834 (4)	3147 (4)	6166 (1)
C(10)	10980 (8)	1825 (7)	6012 (2)	11105 (5)	1957 (5)	6017 (1)
C(11)	8364 (8)	2339 (6)	6453 (2)	8360 (6)	2529 (4)	6411 (1)
C(12)	7170 (8)	3494 (6)	6594 (2)	7191 (5)	3738 (4)	6552 (1)
C(13)	7918 (6)	4763 (6)	6829 (2)	7971 (4)	4991 (4)	6810 (1)
C(14)	9196 (6)	5354 (7)	6498 (2)	9323 (5)	5612 (4)	6514 (1)
C(15)	9606 (8)	6802 (8)	6708 (3)	9763 (6)	7048 (5)	6749 (2)
C(16)	8064 (8)	7363 (8)	6916 (3)	8158 (6)	7705 (4)	6875 (1)
C(17)	6878 (6)	6118 (7)	6877 (2)	6937 (5)	6420 (4)	6862 (1)
C(18)	8579 (8)	4478 (9)	7335 (2)	8546 (6)	4521 (6)	7281 (1)
C(19)	11984 (11)	1245 (11)	6427 (2)	12043 (8)	1271 (7)	6416 (2)
C(20)	5649 (7)	6103 (7)	7271 (2)	5748 (6)	6386 (5)	7254 (1)
C(21)	4166 (9)	5361 (11)	7168 (3)	4198 (7)	5672 (7)	7170 (2)
C(22)	6574 (11)	7733 (9)	6263 (3)	6096 (8)	8252 (5)	6397 (2)
C(23*a*)	4798 (45)	8262 (39)	5996 (14)	6235 (20)	8677 (17)	5884 (5)
C(23*b*)	5357 (18)	8668 (16)	6103 (5)	5460 (15)	8702 (12)	5961 (3)
C(24*a*)	5376 (47)	9400 (42)	5676 (12)	4901 (17)	8251 (16)	5634 (5)

Table 3 (*cont.*)

	(I) in *A*			(II) in *B*		
	x	*y*	*z*	*x*	*y*	*z*
C(24*b*)	4574 (16)	8226 (14)	5662 (5)	6495 (13)	7992 (12)	5576 (4)
C(25*a*)	5446 (19)	8690 (16)	5222 (5)	4964 (20)	8745 (18)	5118 (5)
C(25*b*)				6037 (19)	8646 (17)	5099 (5)
O(3)	11815 (8)	446 (8)	4636 (2)	11873 (6)	823 (6)	4667 (1)
O(11)	9012 (8)	1652 (6)	6860 (2)	8798 (6)	1656 (4)	6796 (1)
O(16)	7366 (7)	8450 (5)	6634 (2)	7620 (5)	8679 (4)	6532 (1)
O(17)	6027 (5)	6408 (5)	6452 (1)	6044 (4)	6694 (3)	6461 (1)
O(20)	5847 (8)	6603 (9)	7637 (2)	6037 (6)	6894 (6)	7627 (1)
O(21)	3058 (7)	5351 (7)	7523 (2)	3229 (7)	5516 (5)	7542 (2)
H(1)	984 (10)	−5 (9)	603 (3)	943 (7)	13 (6)	596 (2)
H(2)	982 (11)	−77 (10)	530 (3)	1001 (6)	−49 (5)	522 (2)
H(4)	1320 (13)	220 (13)	516 (4)	1319 (7)	293 (6)	513 (2)
H(6)	1333 (12)	322 (11)	609 (4)	1370 (6)	373 (6)	615 (2)
H(6)	1361 (13)	428 (11)	564 (3)	1366 (6)	470 (6)	565 (2)
H(7)	1190 (13)	591 (12)	630 (3)	1229 (7)	600 (7)	618 (2)
H(7)	1112 (8)	518 (7)	577 (2)	1165 (6)	557 (6)	577 (2)
H(8)	1109 (8)	397 (8)	676 (2)	1109 (5)	424 (4)	667 (1)
H(9)	904 (7)	310 (6)	585 (2)	934 (7)	350 (6)	588 (2)
H(11)	804 (11)	152 (10)	626 (3)	772 (6)	178 (5)	620 (2)
H(O11)	797 (8)	157 (7)	673 (2)			
H(12)	654 (8)	409 (8)	630 (2)	675 (6)	421 (6)	624 (2)
H(12)	657 (9)	298 (9)	684 (3)	640 (5)	326 (5)	674 (1)
H(14)	856 (11)	540 (10)	620 (3)	890 (4)	588 (3)	625 (1)
H(15)	1035 (11)	660 (10)	686 (3)	1038 (7)	682 (7)	699 (2)
H(15)	991 (11)	752 (10)	647 (3)	1033 (7)	785 (6)	650 (2)
H(16)	825 (9)	750 (7)	730 (2)	814 (6)	808 (5)	720 (2)
H(18)	835 (8)	481 (7)	721 (2)	881 (5)	532 (5)	744 (1)
H(18)	939 (8)	374 (7)	727 (2)	935 (6)	397 (6)	719 (2)
H(18)	797 (9)	394 (8)	744 (2)	778 (5)	412 (5)	743 (1)
H(19)	1239 (12)	242 (11)	651 (3)	1253 (7)	196 (7)	656 (2)
H(19)	1323 (7)	99 (6)	629 (2)	1293 (10)	57 (8)	627 (2)
H(19)	1143 (12)	80 (12)	656 (3)	1163 (10)	85 (9)	661 (2)
H(21)	366 (10)	553 (10)	683 (3)	364 (8)	636 (8)	695 (2)
H(21)	408 (13)	416 (13)	713 (4)	439 (8)	465 (7)	709 (2)
H(O21)	386 (11)	488 (10)	778 (3)	316 (9)	615 (8)	763 (2)
H(22)	762 (6)	798 (5)	592 (2)	532 (11)	870 (9)	650 (3)
H(23*a*)	414	867	623	713	823	576
H(23*a*)	435	753	583	633	974	586
H(23*b*)	582	959	606	546	971	593
H(23*b*)	460	872	636	441	830	592
H(24*a*)	628	979	576	395	870	579
H(24*a*)	453	1012	565	476	721	567
H(24*b*)	354	863	566	640	695	558
H(24*b*)	448	721	566	761	823	565

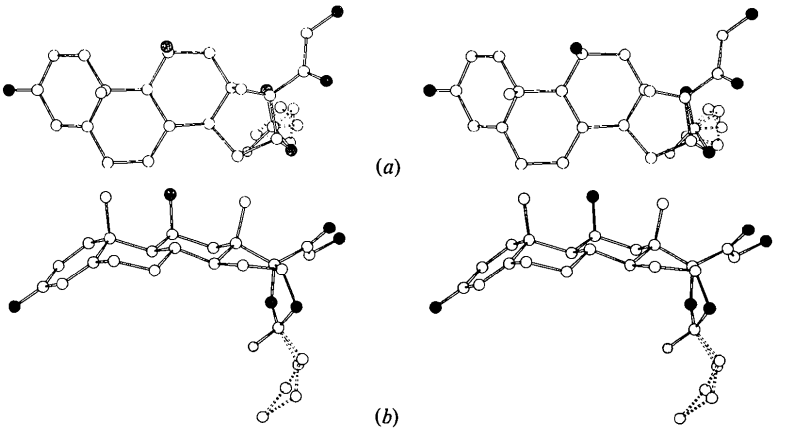

Fig. 2. Stereoscopic pairs of drawings of the molecular skeleton of (I). In (*a*) the molecule is projected on the plane formed by the vectors C(10)—C(13) and C(14)—C(12). In (*b*) the molecule is rotated 77° about C(10)—C(13) compared to the view in (*a*). H(22) is included.

Crystal packing

The molecular structures of (I) and (II) stripped of their H atoms, except H(22), are shown in Figs. 2 and 3 respectively. (I) and (II) are different epimers of budesonide but have almost the same molecular shape, as was discussed in the *Introduction*. Consequently, the crystal packing is very similar in *A* and *B*. Figs. 4 and 5 show projections of the two structures. The highly bent molecules are connected by hydrogen bonds into ribbons, two molecules thick, running parallel to **b** along the twofold screw axes at $x = 0$, $z = \frac{1}{4}$ and $x = \frac{1}{2}$, $z = \frac{3}{4}$. In these ribbons there are only β–β face approaches. The ribbons are stacked along **a**. The outsides of the layers thus formed comprise the α faces of the molecules, so that the *A* rings and the propyl chains of adjacent layers are interlocked by van der Waals contacts. There are fairly large cavities available for the propyl chain in both *A* and *B* making the crystal energy almost equal for at least two possible contact positions. The result is a distribution of the chain between the *a* and *b* positions of Table 3. The orientation of the propyl chain cannot be changed without changes of the conformations of rings *D* and *E* (conformational transmission). The observed geometries of these rings are thus averages of slightly different conformations. Possibly the conformational transmission extends all the way to ring *A* which would explain why this ring is not as well defined as rings *B* and *C*. In both *A* and *B* the crystal packing, the hydrogen-bond system, the propyl-chain conformations and the conformations of the rings are all interdependent. Owing to the large α-axial extension of the propyl chain from the bulk of the steroid molecule the crystal packing in *A* and *B* bears little resemblance to any of the major packing forms observed for steroids (*cf.* Duax & Norton, 1975).

Molecular geometry

Bond distances, bond angles and torsion angles not involving H atoms are listed in Fig. 6(*a*–*c*). The values found for the bond distances and angles in (I) and (II) (excluding the propyl chains) are compared using probability-plot analysis in Fig. 7. Ordered values of δd_i

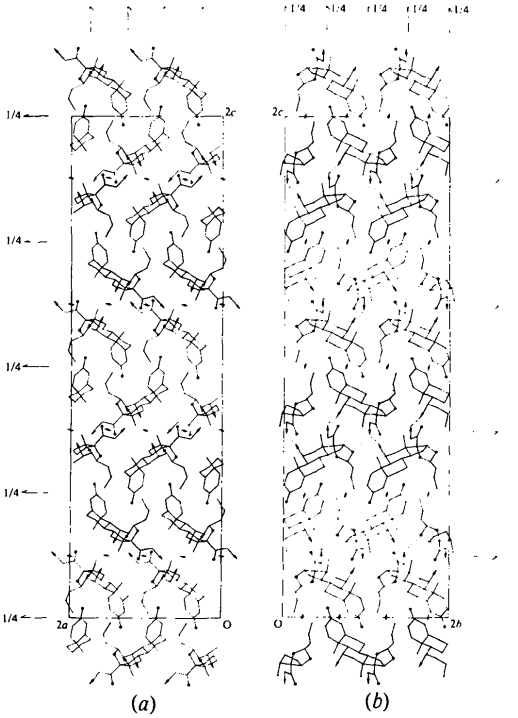

Fig. 4. The packing of epimer (I) in *A*. The contents of four unit cells are shown projected on (*a*) the *ac* plane and (*b*) the *bc* plane. Only the propyl chain with the highest occupancy (0·75) is shown. The dashed lines in (*b*) depict the hydrogen bonds.

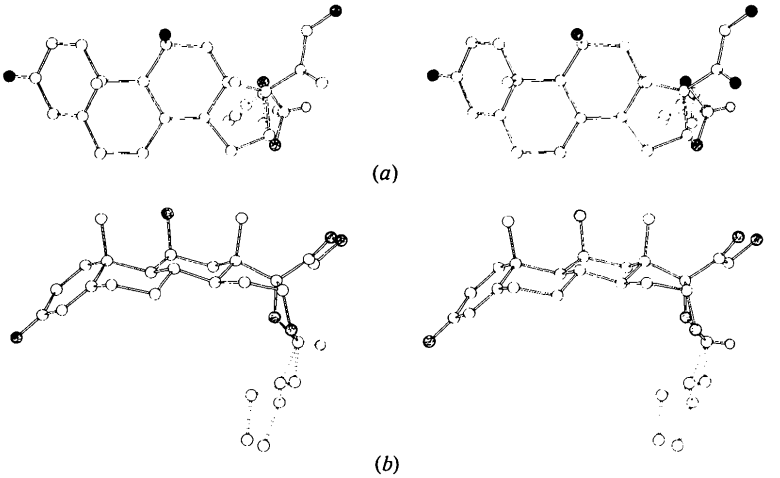

Fig. 3. Stereoscopic pairs of drawings of the molecular skeleton of (II). H(22) is included. The views in (*a*) and (*b*) are the same as those in Fig. 2.

$= |d(\mathrm{I})_i - d(\mathrm{II})_i|/[\sigma^2 d(\mathrm{I})_i + \sigma^2 d(\mathrm{II})_i]^{1/2}$ are plotted *vs* the values expected for a half-normal distribution of zero mean and unit variance (De Camp, 1973; Albertsson & Schultheiss, 1974). Independent interatomic distances $d(\mathrm{I})_i$ and $d(\mathrm{II})_i$ less than 2·50 Å are used. 47 of the 62 δd_i values fall on a straight line with slope 1·7 and intercept −0·03. We conclude that most bond lengths and angles are the same in the two structures and that, on average, the standard deviations in the two structure determinations cannot be underestimated by a factor larger than 1·7. Four bond distances and five bond angles connected to the values of d_i which differ significantly between (I) and (II) are marked with asterisks in Fig. 6(*a*,*b*).

Budesonide shows the same severe strain in the angles C(8)–C(14)–C(15) and C(14)–C(13)–C(17) as do almost all other steroids and the same rather long distances C(9)–C(10) and C(13)–C(17). Comparing the bond lengths and valency angles in (I) and (II) with the average values listed by Duax & Norton (1975) for steroids with 4-ene-3-one constitution, we conclude that where (I) differs from (II) it also differs from the average Δ^4-3-one steroid structure. The determination of (II) in *B* is somewhat better than the determination of (I) in *A*. 820 reflexions were given zero weight for *A* but only 391 were for *B* and the amount of (I) in *B* was less than that of (II) in *A*.

The *E* rings, formed by C(16), C(17), O(17), C(22) and O(16), have no unusual bond distances and angles.

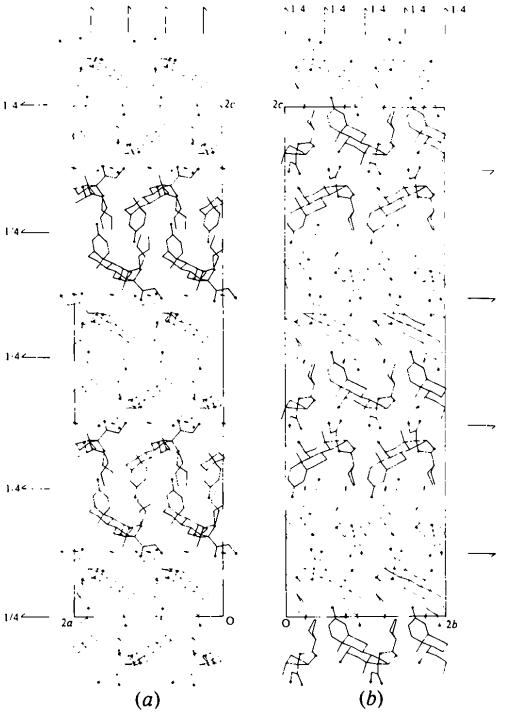

Fig. 5. The packing of epimer (II) in *B*. The same projections as in Fig. 4 are shown.

The observed values agree with those found in other substituted corticosteroids with a similar ring (Thom & Christensen, 1971; Krakower, Keeler & Gougoutas, 1971). Because of the disorder, resulting in overlapping electron densities for C(23) – C(25), the determination of the geometry of the propyl chains is less accurate than for the rest of (I) and (II).

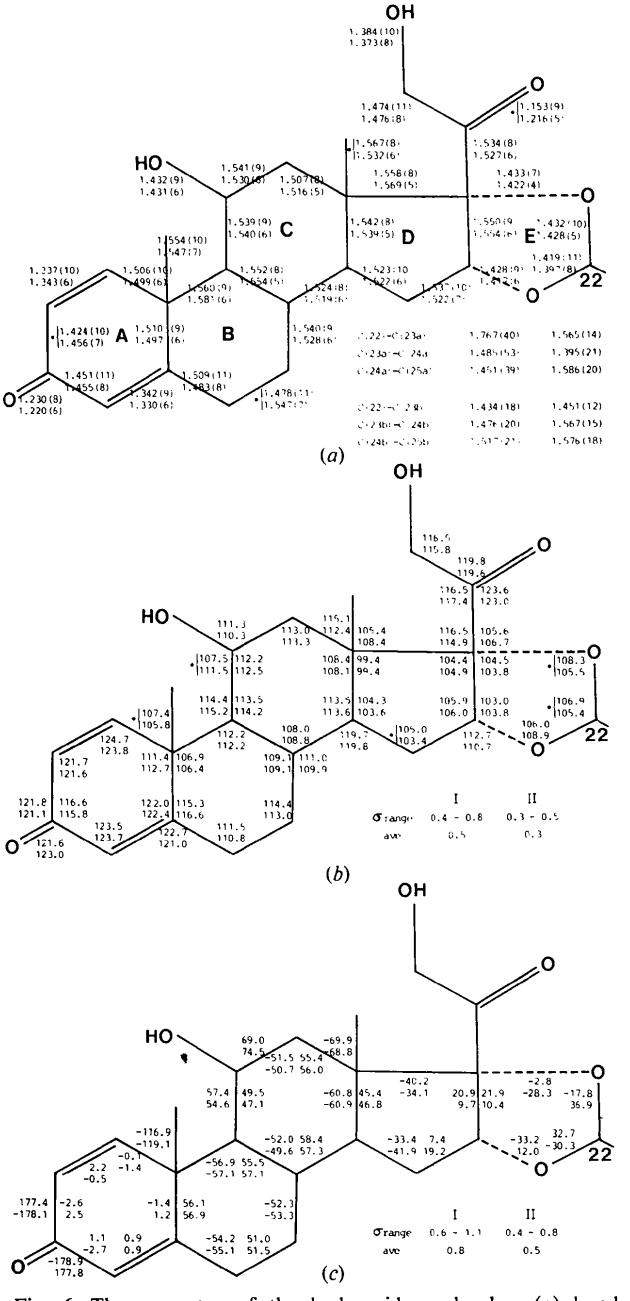

Fig. 6. The geometry of the budesonide molecules: (*a*) bond distances (Å), (*b*) bond angles (°), and (*c*) torsion angles (°). The values for (I) are given above those for (II). In (*a*) and (*b*) asterisks indicate significantly different values. In (*c*) the endocyclic torsion angles are given inside the rings; six exocyclic angles are listed outside the rings. [Atoms C(23) – C(25) are omitted.]

Conformational analysis

In the projections shown in Fig. 8, (I) and (II) are viewed parallel to the least-squares reference plane through the steroid nucleus. The line of sight is approximately along the C(14)–C(12) bond. The bowing of rings *A* and *E* relative to the remainder of the steroid is illustrated. The angle between the normals of ring *A* and the reference plane is 40·7° in (I) and 43·1° in (II). A relationship between the biological activity of corticosteroids and the bowing of ring *A* has been proposed by Weeks, Duax & Wolff (1973). In cortisol (Roberts, Coppola, Isaacs & Kennard, 1973) the angle is 19·8° but in 9α-fluorocortisol (Weeks, Duax & Wolff, 1973), with a much higher anti-inflammatory activity than cortisol, it has increased to 32·5°. Besides 9α fluorination a dehydrogenation of the C(1)–C(2) bond is known to increase the anti-inflammatory activity. The two effects appear to be cumulative. Dexamethasone (Rohrer & Duax, 1977) has both a 9α F atom and a C(1)–C(2) double bond and a very high corticoid activity. The angle between ring *A* and the reference plane is 38·8°. 6α-Methylprednisolone (Declercq, Germain & Van Meerssche, 1972) has the same conjugated 1,4-diene-3-one constitution as dexamethasone and budesonide but, like budesonide, no 9α substituent. The bowing of ring *A* is 36·7°.

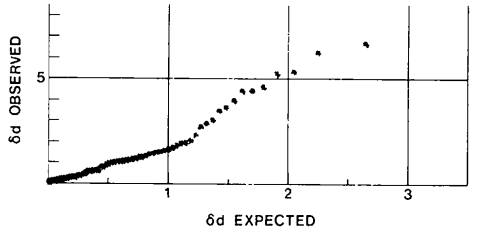

Fig. 7. Half-normal probability-plot comparison of interatomic distances less than 2·50 Å in (I) and (II). The slope is 1·68 and the intercept −0·03 for the 47 points with observed $\delta d < 2{\cdot}0$.

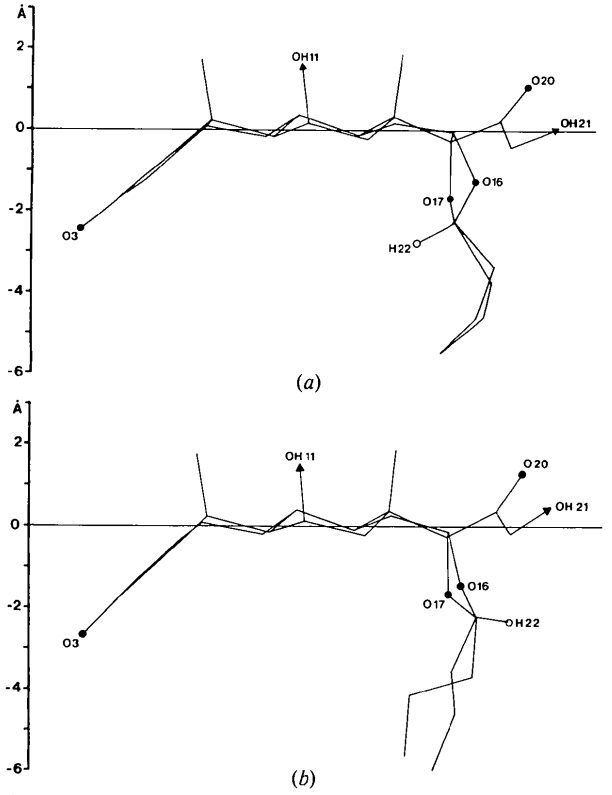

Fig. 8. The conformations of budesonide molecules: projections parallel to the C(5) – C(17) least-squares reference plane; (*a*) epimer (I), (*b*) epimer (II).

The local anti-inflammatory effect of budesonide is much higher than that of cortisol (Thalén & Brattsand, 1978) and probably also higher than those reported for 6α-methylprednisolone and dexamethasone (Dluhy, Newmark, Lauler & Thorn, 1975). Epimer (II), with the larger bowing of ring *A*, is the more active of the two diastereoisomers (Brattsand, Thuresson af Ekenstam, Claesson & Thalén, 1975*b*).

The propylmethylene chain is in the *trans* conformation in (II) but this has changed to the unusual *gauche* in (I) as can be seen in Figs. 1 and 2. It was suspected that this conformation might be favoured by the co-crystallization of (I) and (II) (see below) but

Table 4. *Deviations* (Å) *from the least-squares planes through rings A–E*

Asterisks denote atoms not used in the calculations of the planes.

	(I)	(II)		(I)	(II)
(*a*) Ring *A*					
C(1)	0·00	−0·01	C(5)	−0·01	−0·01
C(2)	−0·01	−0·01	C(10)	0·01	0·01
C(3)	0·01	0·02	*C(6)	−0·08	0·07
C(4)	0·00	−0·01	*O(3)	0·05	0·05
(*b*) Ring *B*					
C(5)	0·02	0·01	C(8)	0·01	0·01
C(10)	−0·01	−0·01	*C(6)	−0·60	−0·63
C(7)	−0·02	−0·01	*C(9)	0·68	0·70
(*c*) Ring *C*					
C(8)	−0·01	−0·02	*C(11)	−0·61	−0·59
C(9)	0·01	0·02	*C(14)	0·69	0·68
C(12)	−0·01	−0·02	*O(11)	2·02	2·02
C(13)	0·01	0·02			
(*d*) Ring *D*					
C(14)	−0·03	−0·07	*C(13)	0·68	0·66
C(15)	0·04	0·11	*C(18)	2·20	2·17
C(16)	−0·04	−0·11	*O(17)	−1·34	−1·25
C(17)	0·03	0·07			

(*e*) Ring *E*

C(16)	−0·01	C(16)	−0·06	C(22)	0·01	O(17)	−0·04
C(17)	0·02	O(16)	0·04	*O(16)	0·47	*C(22)	0·47
O(17)	−0·02	C(17)	0·06				

Table 5. *Asymmetry parameters* (°) (*Duax & Norton*, 1975) *and average endocyclic dihedral angles* (°) *for rings B and C*

	Most ideal symmetry	Next highest symmetry	Parameter for symmetry orthogonal to most ideal symmetry	Average endocyclic dihedral angle
Ring *B* (I)	$\Delta C_s^7 = 1{\cdot}2$	$\Delta C_2^{6,7} = 1{\cdot}4$	$\Delta C_s^5 = 4{\cdot}0$	54·3
(II)	$\Delta C_2^{6,7} = 1{\cdot}3$	$\Delta C_s^7 = 1{\cdot}6$	$\Delta C_s^5 = 4{\cdot}0$	55·2
Ring *C* (I)	$\Delta C_2^{9,11} = 2{\cdot}2$	$\Delta C_s^{11} = 2{\cdot}7$	$\Delta C_s^8 = 7{\cdot}8$	54·6
(II)	$\Delta C_2^{9,11} = 1{\cdot}2$	$\Delta C_s^{11} = 4{\cdot}7$	$\Delta C_s^8 = 9{\cdot}6$	53·6

even very pure (I) crystallized with the same unit cell (Table 1) and thus the same molecular packing as *A*. In both epimers this substituent is equatorial to ring *E*. As ring *E* is bent 87° from the reference plane in (I) and 75° in (II), the propyl chains are α-axial to the steroid nuclei. They extend about 6 Å from the reference planes.

Ring *A* is planar as required by its conjugated bond system, with C(6) of ring *B* in the plane of ring *A*. Table 4(*a*) gives the deviations of relevant atoms from the least-squares plane through the six C atoms forming ring *A*.

Rings *B* and *C* both have chair conformations. Following Duax & Norton (1975) we have calculated the asymmetry parameters ΔC_s^k and $\Delta C_2^{k,l}$. The parameter which has the lowest magnitude indicates the most ideal symmetry. Table 5 gives some ΔC values for rings *B* and *C*. In both (I) and (II) the dominant symmetries of the ring *B* chair are the twofold axis intersecting the C(6)–C(7) and the C(9)–C(10) bonds, and the mirror plane through C(7) and C(10). In (I) the dominant symmetries of the ring *C* chair are the twofold axis intersecting the C(9)–C(11) and C(13)–C(14) bonds and the mirror plane through C(11) and C(14). In (II) the twofold axis alone dominates ring *C* symmetry. The average values of the endocyclic dihedral angles in each *B* and *C* ring are also given in Table 5. The puckering of these rings is described by the deviations from the least-squares planes, as listed in Table 4(*b*) and (*c*).

Ring *D* is a 13β,14α-half chair, distorted towards a 13β-envelope in (I) and towards a 14α-envelope in (II). The pseudorotation parameters (Altona, Geise & Romers, 1968) are (I): $\Delta = 16{\cdot}5°$, $\varphi_{max} = 45{\cdot}9°$; (II): $\Delta = -13{\cdot}7°$, $\varphi_{max} = 47{\cdot}1°$. The deviations from the least-squares planes through C(14), C(15), C(16) and C(17) are given in Table 4(*d*). Ring *E* is an O(16)-envelope in (I) ($\Delta = -28{\cdot}3°$, $\varphi_{max} = 34{\cdot}2°$) but in (II) its conformation is an O(17),C(22)-half chair ($\Delta = 3{\cdot}6°$, $\varphi_{max} = 36{\cdot}9°$). Table 4(*e*) lists the deviations from the least-squares planes. The different conformations of rings *D* and *E* in (I) and (II) can also, of course, be seen in their different torsion angles, as listed in Fig. 6(*c*).

Table 6. *Some torsion angles* (°) *for the* 17β *side chain and the ring junctions*

	(I)	(II)
(*a*) 17β side chain		
C(13)–C(17)–C(20)–O(20)	92·2 (8)	94·7 (5)
C(13)–C(17)–C(20)–C(21)	−81·9 (7)	−84·1 (5)
C(17)–C(20)–C(21)–O(21)	−179·9 (6)	173·1 (5)
O(20)–C(20)–C(21)–O(21)	2·0 (1·0)	−5·8 (8)
C(18)–C(13)–C(17)–C(20)	−51·1 (6)	−44·1 (4)
(*b*) *A*/*B* junction		
C(1)–C(10)–C(5)–C(6)	176·9 (6)	177·6 (4)
C(4)–C(5)–C(10)–C(9)	−122·3 (7)	−119·5 (5)
(*c*) *B*/*C* junction		
C(10)–C(9)–C(8)–C(14)	176·3 (5)	177·0 (3)
C(7)–C(8)–C(9)–C(11)	−172·8 (5)	−169·5 (3)
(*d*) *C*/*D* junction		
C(12)–C(13)–C(14)–C(15)	167·2 (5)	167·6 (3)
C(8)–C(14)–C(13)–C(17)	177·4 (5)	178·3 (3)
(*e*) *D*/*E* junction		
C(13)–C(17)–C(16)–O(16)	139·4 (5)	126·7 (3)
C(15)–C(16)–C(17)–O(17)	−96·6 (6)	−106·6 (4)

The atoms of the 17β side chain are coplanar. Table 6 gives some torsion angles for this chain and the ring junctions. The torsion angles C(13)–C(17)–C(20)–C(21) and C(18)–C(13)–C(17)–C(20) have the values expected for 17α-acetoxy and 21-hydroxy substituents (Duax & Norton, 1975). The C(20)–O(20) keto bond is oriented over ring *D* anticlinal to C(13)–C(17). The *A*/*B* ring junction is planar as required by the trigonal C(5) atom and the planar ring *A*. The *B*/*C* and *C*/*D* ring junctions are both *trans* while the *D*/*E* junction is *cis*. Of the functional groups, C(18), C(19) and O(11) are β-axial, O(16) and O(17) are α-axial and O(3) is equatorial. The distances between the functional O atoms in the molecule are given in Table 7.

The formation of solid solutions

The hydrogen bonds linking the budesonide molecules into ribbons as shown in Figs. 4 and 5 are formed between O(11), O(16) and O(21). In both the structures

investigated (*A* and *B*) an O(11)···O(21) bond connects adjacent molecules. A third molecule is linked to this pair *via* a weak bond: O(16)···O(21) in *A* and O(11)···O(16) in *B*, as depicted in Fig. 9. This bonding scheme is deduced from the O···O distances and the positions of the H(O21) atoms.

The dimensions of the two triangular hydrogen-bond systems are similar. One hydrogen-bond triangle can be reversed without a severe reaction in the other hydrogen bonds. In *A* (epimer I) O(16) and O(21) are the hydrogen-bond acceptors but in *B* (II) the acceptors are O(11) and O(16). Since the dimensions of (I) and (II) are very similar, as are the unit cells of *A* and *B*, it is a matter of course to assume that the two epimers can pack together in the same crystal with a variable composition from pure (I) to pure (II). However, a complete phase analysis of the binary system (I)–(II) cannot be made. The compounds decompose on melting so the liquidus curve cannot be determined (Thalén & Wickström, 1977). In most cases there are also very few lines visible in the powder X-ray photographs. As a result our conclusions regarding the

Table 7. *Intramolecular distances* (Å) *between the functional* O *atoms*

	(I)	(II)		(I)	(II)
O(3)–O(11)	6·85	6·84	O(11)–O(21)	6·45	6·26
O(3)–O(16)	10·17	9·70	O(16)–O(17)	2·29	2·25
O(3)–O(17)	9·08	8·98	O(16)–O(20)	3·58	3·85
O(3)–O(20)	11·50	11·44	O(16)–O(21)	5·33	5·55
O(3)–O(21)	12·02	11·97	O(17)–O(20)	3·37	3·45
O(11)–O(16)	6·58	6·52	O(17)–O(21)	4·08	4·12
O(11)–O(17)	5·28	5·23	O(20)–O(21)	2·68	2·69
O(11)–O(20)	5·82	5·84			

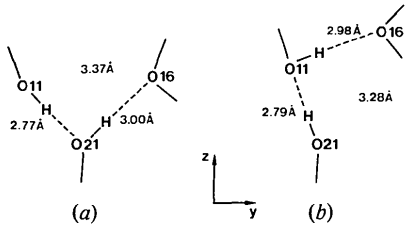

Fig. 9. Proposed hydrogen bonds in (*a*) preparation *A* and (*b*) preparation *B* of budesonide.

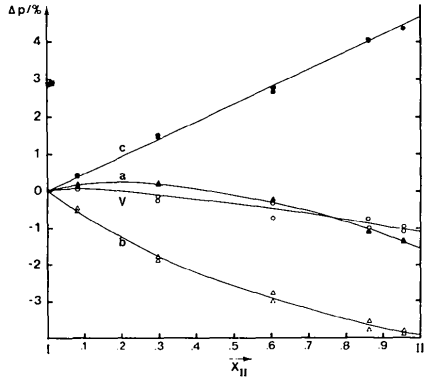

Fig. 10. The variations of the unit-cell dimensions of budesonide as a function of the epimeric composition (*cf.* Table 1).

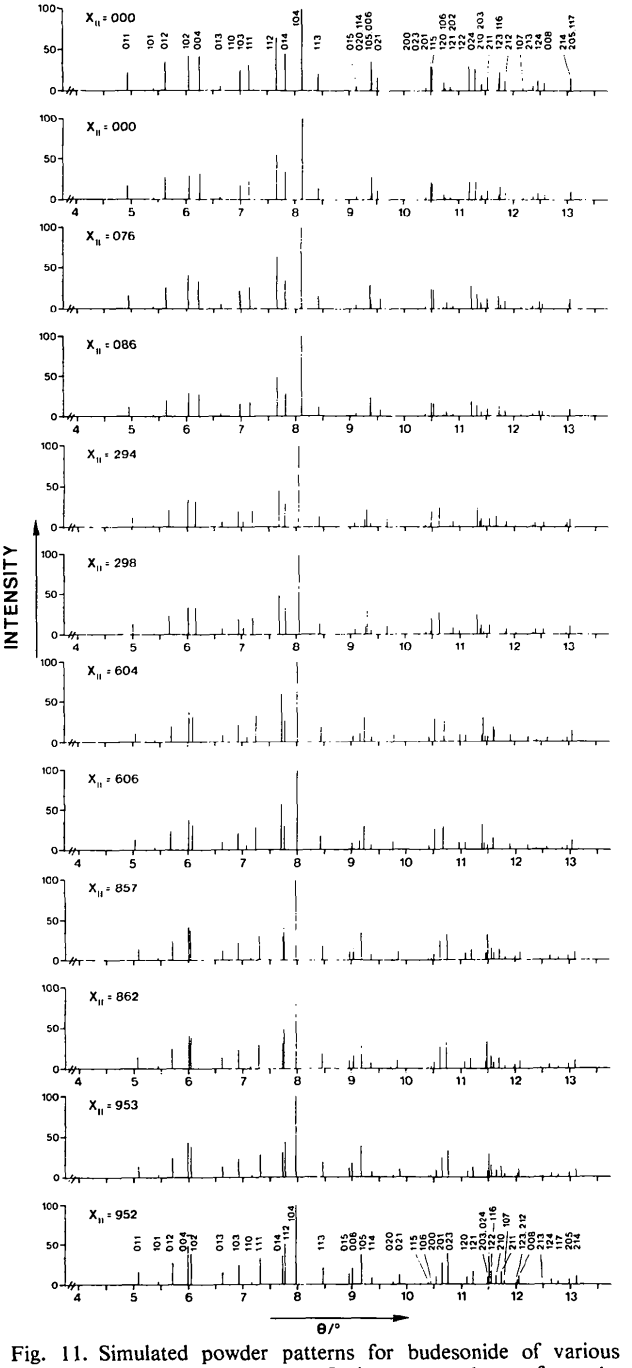

Fig. 11. Simulated powder patterns for budesonide of various epimeric compositions. The reflexions were chosen from the powder patterns of *A* and *B* and the intensities were determined with single crystals on a CAD-4 diffractometer.

possible phases of budesonide are based on the investigations of the twelve single crystals described in Table 1.

Fig. 10 shows the variation in the unit-cell dimensions given in Table 1. While c increases about 5% when the epimeric composition goes from pure (I) to pure (II), b decreases about 4% and a about 1·5%. Consequently, the value of the unit-cell volume is fairly constant. The intensities of the low-angle reflexions used in the determination of the cell constants are shown in Fig. 11. The variation of the cell dimensions causes small shifts in the relative positions of many reflexions (*e.g.* between 102 and 004 and between 112 and 014), but very few disappear or arise which would be the case if different phases were formed. The distribution of the intensity over the various reflexions is also nearly the same in the six preparations. However, comparison of the powder photographs of *A* and *B* alone did not immediately reveal that the crystals are isomorphous.

Inclusion of both (I) and (II) in the same crystal must give rise to some disorder; this is most pronounced at $x_{II} = 0{\cdot}5$ if new phases are not formed. Such a disorder should show up in a broadening of the peak profiles (James, 1965). Fig. 12 shows the average peak width in the θ interval 5·1–13·2° plotted *vs* the epimeric composition. The resulting curve appears to have a maximum at $x_{II} = 0{\cdot}5$ where the width is about four times greater than those for pure (I) and (II). This shape is consistent with the co-crystallization of (I) and (II) in a structure where the molecular positions on the unit-cell level are randomly occupied by (I) and (II). Taken together, Figs. 10–12 strongly suggest that the two epimers of budesonide form a continuous range of solid solutions.

We thank Dr A. Wikby, AB Draco, for suggesting the investigation and Dr B. A. Thalén for the steroid preparations and single crystals placed at our disposal.

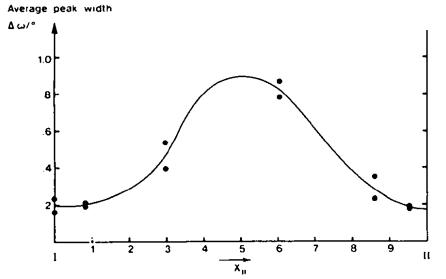

Fig. 12. The average peak width for a reflexion from budesonide as a function of the epimeric composition. The average values were calculated from the peak profiles in the θ range 5·1–13·2° (*cf.* Fig. 11).

We are indebted to them and to Mr S. Hugosson for many valuable discussions. We also thank Mrs B. Briggman and Mrs M. Molund for help with part of the experimental work and for the preparation of the illustrations.

References

ALBERTSSON, J. & SCHULTHEISS, P. M. (1974). *Acta Cryst.* A**30**, 854–855.

ALTONA, C., GEISE, H. J. & ROMERS, C. (1968). *Tetrahedron*, **24**, 13–32.

BRATTSAND, R. L., THURESSON AF EKENSTAM, B., CLAESON, K. B. & THALÉN, B. A. (1975*a*). US patent 3 929 768.

BRATTSAND, R. L., THURESSON AF EKENSTAM, B., CLAESON, K. B. & THALÉN, B. A. (1975*b*). US patent 3 938 326.

DANIELSSON, S., GRENTHE, I. & OSKARSSON, Å. (1976). *J. Appl. Cryst.* **9**, 14–17.

DE CAMP, W. H. (1973). *Acta Cryst.* A**29**, 148–150.

DECLERCQ, J. P., GERMAIN, G. & VAN MEERSSCHE, M. (1972). *Cryst. Struct. Commun.* **1**, 5–7.

DLUHY, R. G., NEWMARK, S. R., LAULER, D. P. & THORN, G. W. (1975). *Steroid Therapy*, edited by D. L. AZARNOFF, pp. 1–14. Philadelphia: Saunders.

DOYLE, P. A. & TURNER, P. S. (1968). *Acta Cryst.* A**24**, 390–397.

DUAX, W. L. & NORTON, D. A. (1975). Editors, *Atlas of Steroid Structure.* Vol. 1. New York: Plenum.

GERMAIN, G., MAIN, P. & WOOLFSON, M. M. (1971). *Acta Cryst.* A**27**, 368–376.

JAMES, R. W. (1965). *The Optical Principles of the Diffraction of X-rays*, pp. 555–560. London: Bell.

KRAKOWER, G. W., KEELER, B. T. & GOUGOUTAS, J. Z. (1971). *Tetrahedron Lett.* **4**, 291–294.

ROBERTS, R. J., COPPOLA, J. C., ISAACS, N. W. & KENNARD, O. (1973). *J. Chem. Soc. Perkin Trans.* 2, pp. 774–781.

ROHRER, D. C. & DUAX, W. L. (1977). *Cryst. Struct. Commun.* **6**, 123–126.

STEWART, R. F., DAVIDSON, E. R. & SIMPSON, W. T. (1965). *J. Chem. Phys.* **42**, 3175–3187.

THALÉN, B. A. & BRATTSAND, R. L. (1978). *Arzneim. Forsch.* In the press.

THALÉN, B. A. & WICKSTRÖM, L.-I. (1977). Private communication.

THOM, E. & CHRISTENSEN, A. T. (1971). *Acta Cryst.* B**27**, 573–581.

WEEKS, C. M., DUAX, W. L. & WOLFF, M. E. (1973). *J. Am. Chem. Soc.* **95**, 2865–2868.

WIKBY, A., NILSSON, L. & HÄLLSÅS, G. (1978). *J. Chromatogr.* In the press.

WIKBY, A., THALÉN, B. A. & ORESTEN, G. (1978). *J. Chromatogr.* In the press.

ZACHARIASEN, W. H. (1967). *Acta Cryst.* **23**, 558–564.